Int. J. Electrochem. Sci., 13 **(2018)** 10548 – 10563, doi: 10.20964/2018.11.19

International Journal of
ELECTROCHEMICAL
SCIENCE
www.electrochemsci.org

Study on Mechanical Properties of Acidic and Alkaline Silty Soil by Electrochemical Impedance Spectroscopy

Peng Han, Pengju Han, Yibo Yan, Xiaohong Bai*

Tianjin University, State Key Lab Hydraul Engn Simulat & Safety, TianJin 300350, Peoples R China
*E-mail: 13834569544@163.com

Received: 23 July 2018 / *Accepted:* 23 August 2018 / *Published:* 1 October 2018

In this study, Electrochemical Impedance Spectroscopy (EIS) was used to test H_2SO_4 and NaOH contaminated silty soil. To further study the mechanical properties (shear strength and compressive properties) of contaminated silty soil, an equivalent circuit model (R_s (CPE (R_t R_w))) was established to simulate the changes in silty soil contaminated by various concentrations of H_2SO_4 and NaOH solutions. Experiments showed that with the increase in the amount of acid-base contaminant involved, the shear strength of the contaminated silty soil decreased, and the compressive properties increased. By analysing the equivalent circuit model, it can be observed that with the increase in the amount of acid-base contaminant involved, the solution resistance R_s and charge transfer resistance R_t decreased, while the diffusion admittance Y_{OW} and double layer admittance Y_{OQ} increased. Of these, R_t and Y_{OW} vary significantly, indicating that the resistance of the charge transfer process and diffusion process are considerably reduced, and the electrochemical reaction becomes easier. As a result, more and more minerals in the silty soil medium become soft plastic products during the electrochemical reaction. Simultaneously, various organic and inorganic cement materials between the soil particles are dissolved, and the connection between the silty soil particles is weakened. Eventually, the compressibility of silty soil increases and the shear strength is considerably reduced.

Keywords: silty soil, shear strength, compressive properties, EIS

1. INTRODUCTION

Soil is a natural product deposited by rocks under the long-term geological effects of weathering and denudation, and is also transported by wind and water. Soil is composed of three phases (solid, liquid and gas) and has a noticeable impact on human life, mainly in the fields of architecture and agriculture. In recent time, with rapid industrial development in China, the problem of environmental pollution is becoming increasingly serious. The industrial wastewater generated in modern industrial production processes has infiltrated the soil layer because of disorganized discharge

and failure in the discharge system. As a result, the physical, mechanical and chemical properties of the soil have changed considerably. Among these changes, the attenuation of mechanical properties of contaminated soil may cause considerable losses to engineering construction; e.g., in some small paper mills, due to the lack of capital and technology, wastewater (mainly waste alkali liquid) that is directly discharged into nearby rivers and lakes, penetrates into the foundation soil of neighbouring building, and the strength of the foundation is reduced, which is likely to cause instability. Similarly, in the central and eastern part of China, acid rain caused by environmental pollution is becoming increasingly severe. Acid rain permeates into the soil and destroys the soil structure, which may reduce the bearing capacity of the foundation soil and have a significant impact on the stability of the building. Therefore, soil contamination needs to be carefully studied.

Several scholars have studied contaminated soil, mainly from two perspectives. One is to study the corrosiveness of the contaminated soil, and the second is to study the change in the physical and mechanical properties of the contaminated soil. Among them, research on the corrosiveness of contaminated soil has been relatively comprehensive. The researchers simulated the contaminated soil of the actual project by introducing erosive ions into soil and soil-simulated solutions, or by changing soil moisture, temperature, salt content, heavy metal content, pH value, and microbial content[1-10]. A considerable amount of research has also been conducted on the corrosiveness of different types of contaminated soil, i.e., silt, clay and sand[11-13]. Simultaneously, research methods adopted to study the corrosivity of the contaminated soil from the perspective of construction are also varied, such as electrochemical impedance testing, polarization curve, electrical resistance sensor, weightlessness, electrochemical noise and other testing methods[14-20].Although some progress has been made in researching the properties of contaminated soil, in the field of civil engineering, it is still limited to exploring the changes in the dry density, plastic limit index, pore ratio and other physical properties as well as the shear strength and compressibility of contaminated soil through indoor experiments, which are time-consuming and complicated. In this study, the Electrochemical Impedance Spectroscopy (EIS) technique is used to establish an equivalent circuit model. By using the components of capacitance, inductance and resistance in the circuit, the ion diffusion activity, the changes in electrode potential and the process of charge transfer are characterized. Thus, a low-cost, quick and effective detection method for the changes in the mechanical properties of contaminated soil is provided. Electrochemical methods are widely used in the testing of concrete properties. For example, the equivalent circuit model is used to analyse the hydration time of dry cement mortar[21, 22]. At present, studies on the changes in the mechanical properties of contaminated soil by electrochemical methods can adopt one of two directions. One is the qualitative analysis of the electrochemical impedance spectroscopy (Nyquist and Bode)[23], and the other is the establishment of the equivalent circuit diagram to analyse the trend of the components quantitatively[24]. However, many studies do not systematically point out the physical meaning of electrochemical components. By analysing the variation tendency of the capacitance and resistance in the equivalent circuit element and combining the changes in the mechanical properties of the contaminated soil, this study tries to use the equivalent circuit model to explain the mechanism of the mechanical properties of contaminated soil.

2. EXPERIMENTAL

2.1 Experimental materials and pre-treatment

The soil samples used in this experiment were widely distributed in China. The soil was taken from a construction site in Shanxi province of China and was filtered through a 2.5 mm sieve. The particle analysis results are presented in Table 1. The basic physical indicators of the test soil are listed in Table 2. It can be seen from Table 1 and Table 2 that, according to national standards, the soil sample belongs to silty soil. The water content is 1.36%. Its physical and mechanical properties are between sand and cohesive soil. The application of silty soil is quite extensive in engineering practice. Therefore, the selection of silty soil as a research object has a certain representativeness.

Table 1. Particle analysis results

Particle size (mm)	2.25-0.075	0.075-0.05	0.05-0.01	0.01-0.005	<0.005
Content (%)	29	33.8	30.5	2.6	4.1

Table 2. Physical properties of silty soil

Uniformity coefficient	3.78	Liquid limit (W_L)	23.9%
Coefficient of curvature	1.58	Plastic limit (W_P)	17.8%
Specific gravity	2.69	Plasticity index	6.1

In this experiment, silty soil was contaminated by various concentrations of H_2SO_4 and NaOH solution, and contaminated soil was used to simulate actual engineering. H_2SO_4 and NaOH solution are the most common soil pollutants. Taking them as research objects has a certain engineering significance. The acid and alkali used in this experiment are 98% concentrated sulfuric acid (Taiyuan Chemical Co., Ltd.) and sodium hydroxide, which is more than 96% pure (produced by Tianjin co-M). The optimal moisture content of silty soil can be determined to be 16% by compaction curves. Under the premise of ensuring a water content of 16%, acid-base solution of different concentration and the silty sample were uniformly mixed by manual stirring. According to the "Soil Test Method Standard" (GB_T50123-1999), the PHS-3C pH metre (Shanghai Lei Magnetic Co., Ltd.) was used to test the pH value of the contaminated silty soil. Eventually, five sets of representative powders with different pH value were selected. The proportion of contaminated silty soil in each group is listed in Table 3.

Table 3. The preparation content of each silty soil sample

Group	pH=2.8	pH=5.4	pH=7.0	pH=9.3	pH=12.4
H_2SO_4/ml	37.1	7.4	-	-	-
NaOH/g	-	-	-	0.74	14.70
H_2O/ml	73.5	73.5	73.5	73.5	73.5
Silty soil/g	500	500	500	500	500
Water content/%	16	16	16	16	16

2.2 Test and characterization

2.2.1 Mechanical test

The mechanical tests of soil include the quick shear test and compression test, which are used to test the shear strength and compression performance of silty soil. In this study, the ZJ strain direct shear apparatus was used to test the shear strength of contaminated silty soil with various pH values. The shear rate of the instrument is 8mm/min, and its measuring ring coefficient is C=248 kPa·mm^2. The curves of shear strength τ relative to vertical pressure P_v can be obtained experimentally. And the shear strength index of soil was calculated by these curves and Kulun formula, including cohesive force c and internal friction angle φ. The compression curve (e-p) of contaminated silty soil with various pH values was obtained by using a WG single lever consolidating instrument through lateral confining compression test. The compression coefficient (a), compression index (C_c) and compression modulus (E_s) are three indicators to characterize the compressibility of soil, which can be obtained by e-p curves.

2.2.2 Electrochemical test

In this experiment, the CS350 electrochemical workstation (Wuhan Coast) was used to conduct EIS of contaminated silty soil. The amplitude of the AC sine signal of the instrument is 10mV, and the test frequency is 10^{-2}~10^5Hz. The mould used in this test is made of toughened glass material, which is divided into three layers in the left, middle and right. The left and right sides are attached with copper as the electrode, while the hollowed part of the middle layer has a fixed function on the soil sample.

A two-electrode system was used to test the EIS of contaminated soil. The soil sample is placed in the mould, and the ends of the left and right mould are each attached to the copper sheet with a diameter of 60 mm. The connecting wires on the copper sheet are respectively connected with the workstation wire clamp. One end of the wire is connected to the working electrode (WE), and the reference electrode (RE) and the auxiliary electrode (CE) are connected to the other end wire. A closed loop was formed between the soil sample and the electrochemical workstation.

3. RESULTS AND DISCUSSION

3.1 Mechanical properties of contaminated silty soil

3.1.1 Shear resistance of contaminated silty soil

The shear strength of five sets of contaminated silty soil samples under different loads (100 kPa, 200 kPa, 300 kPa and 400 kPa) was tested. The τ-P_v line chart was obtained by using the vertical load, P_v, and the shear strength of soil, τ, as abscissa and ordinate respectively, as shown in Fig. 1. In the lateral dimension, it can be seen from Fig. 1 that the shear strength of each silty soil sample increases with the increase in vertical load. In the longitudinal dimension, the shear strength of the silty

soil with a pH value of 7.0 is higher than that of others, and the shear strength decreases as the pH value of the contaminated silty soil deviates from 7.0. The shear strength of the silty soil decreases with the increase in the pH value deviating from 7.0. This may be because with the increase of the external load, the void volume in the soil decreases significantly, the biting force between the soil particles increases, the soil structure was more compact, and the ability to resist shear deformation is enhanced. In addition, under the fixed vertical load, with the continuous intervention of the acid and alkali pollutants,the shear strength is reduced.

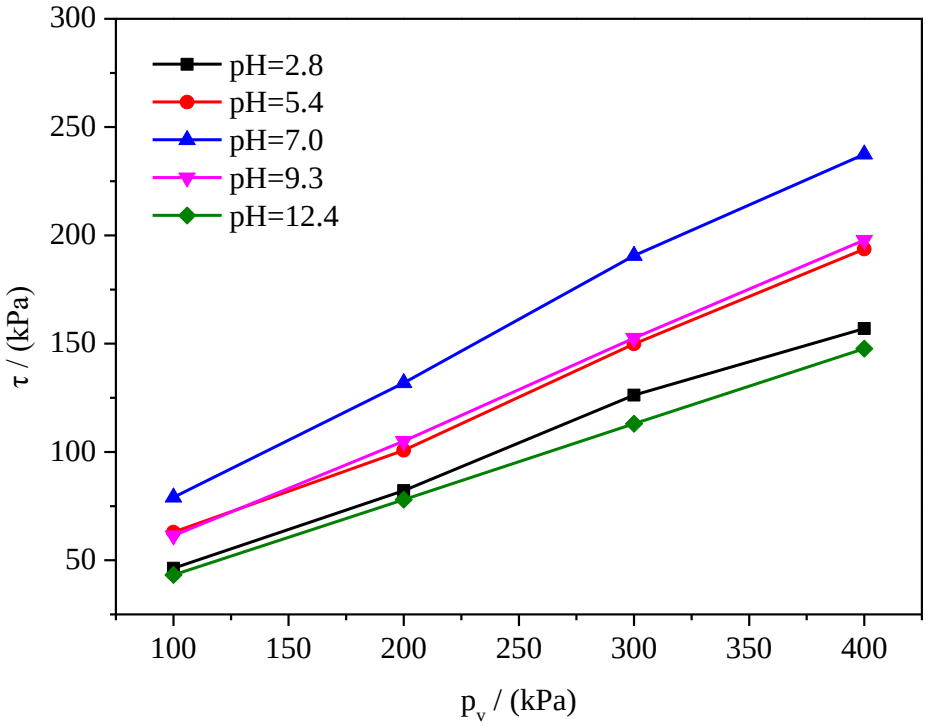

Figure 1. Relationship between shear strength (τ) and vertical pressure (P_v= 100 kPa, 200 kPa, 300 kPa and 400 kPa) of soil with various pH values (pH = 2.8, 5.4, 7.0, 9.3 and 12.4)

The shear strength is actually controlled by two parameters, namely internal friction angle φ and cohesive force c. φ represents the internal friction of the silty soil, which is mainly composed of the friction and the cohesion of the silty soil particles. c is mainly composed of van der Waals force, electrostatic force and cementation force between soil particles. φ and c of silty soil with different pH values can be obtained by τ-P_v curves (as shown in Fig. 1). . Fig. 2 is a line chart of c and φ with the change of pH values of silty soil. It can be seen from the figure that the influence of pH values on c and τ is that when the silty soil is acid (pH <7.0), c and φ increase with the increase of the pH values. When the pH value of the silty soil is 7.0, c and φ reach the maximum.When the silty soil is alkaline (pH value >7.0), the c and φ decrease with the increase of pH values, and reach the minimum when the pH value of silty soil is 12.4.

The variation of c and φ shown that the soil structure was disturbed by an increasing number of involvement of aggressive ions. A series of electrochemical reactions occurred in contaminated silty soil medium. As a result, van der Waals force, electrostatic force and cementation force between molecules decreased. The bonding force (friction and cohesion) between the soil particles was weakened. Therefore, the silty soil was easily fractured and the capacity of shear strength decreased[32].

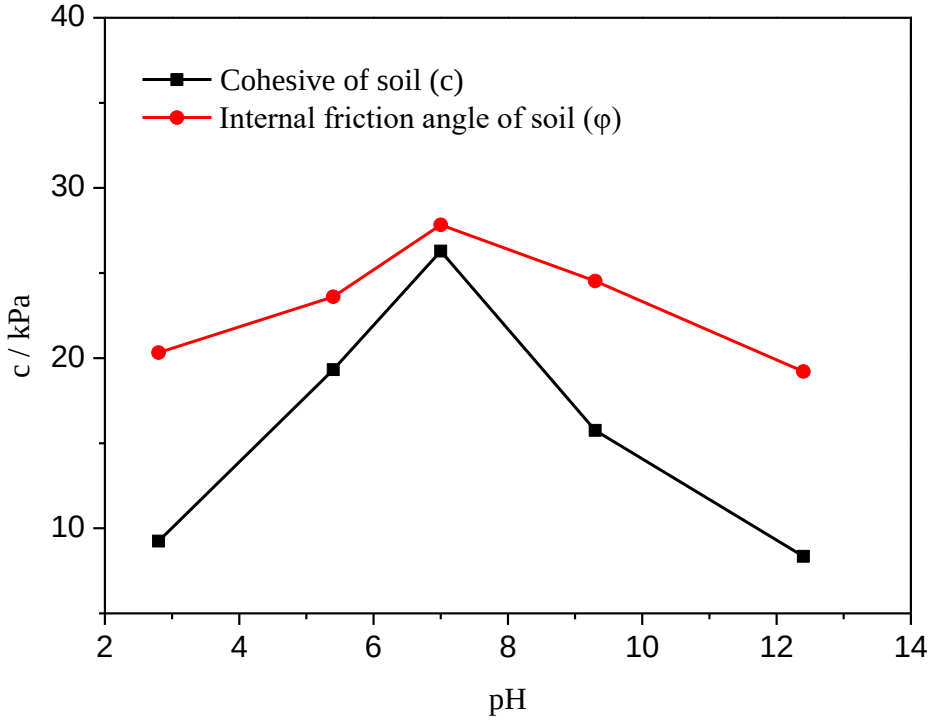

Figure 2. Cohesive and internal friction angle of soil with various pH values (pH = 2.8, 5.4, 7.0, 9.3 and 12.4)

3.1.2 Compressibility of contaminated silty soil

The compression curve of silty soil is a graphic description of the change process of the pore volume under vertical loading at different levels. The loading sequence of this experiment is 25 kPa, 50 kPa, 100 kPa, 200 kPa, 400 kPa, 800 kPa, 1600 kPa and 3200 kPa. The corresponding void ratio can be calculated according to the deformation of each soil sample under different loads. Fig. 3 is the compression curve (e-p) of silty soil with various pH values based on the load as the abscissa and the silty soil void ratio as the ordinate. It can be seen from the figure that the void ratio of each silty soil sample decreases with increasing external load. When the load reaches 400 kPa, the descending trend of silty soil void ratio begins to slow down, especially for the silty soil sample with pH value of 7.0. When the load reaches 1600 kPa, the decline rate of silty soil void ratio continues to slow down, and the void ratio of silty soil sample with pH value of 7.0 tends to be stable. Vertically, at 0 kPa, the initial pore ratio of silty soil with a pH value of 7.0 is the lowest. With the change in the neutral silty soil to

strong acid or strong alkaline, the pore ratio of the silty soil sample increases continuously. When the loading range is 400~1600 kPa, the decrease in the void ratio of silty soil is as follows: the silty soil with pH value of 2.8 and 12.4 has the largest decrease, and the silty soil with pH value of 5.4 and 9.3 is second, and the silty soil with the pH value of 7.0 has the smallest decrease. The same change also appears in the loading range of 1600~3200 kPa.

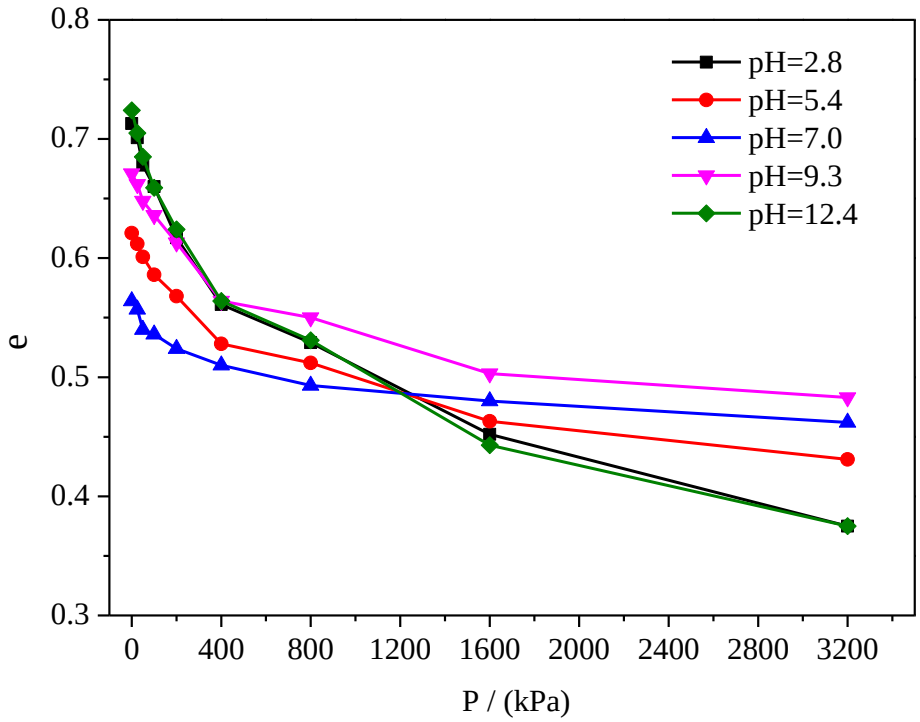

Figure 3. The e-p curve of contaminated silt with various pH values (pH = 2.8, 5.4, 7.0, 9.3 and 12.4)

To intuitively characterize the final change in the void ratio of the contaminated silty soil after loading, the value of final void ratio change Δe (Δe = e_0 - e_{3200}) is calculated according to the Fig.3, and the results are listed in Table 4. It can be clearly seen from Table 4 that when the external load is from 0 kPa to 3200 kPa, the value of Δe of contaminated silty soil with a pH value of 7.0 is the smallest. When the pH value of silty soil is less than 7.0, Δe increases with the decrease in pH values. Δe increases with the increase in pH values while the pH value of silty soil is higher than 7.0.

Table 4. Final reduction (Δe = e_0 - e_{3200}) of void ratio of silt with various pH value

Group	pH=2.8	pH=5.4	pH=7.0	pH=9.3	pH=12.4
e_0	0.713	0.621	0.564	0.671	0.724
e_{3200}	0.375	0.431	0.462	0.483	0.375
Δe	0.358	0.191	0.102	0.187	0.349

According to the compression curve (e-p), three indexes used for evaluating the compressibility of silty soil are obtained; the compression coefficient a, the compression modulus E_s and the compression index C_c. The relationship between the three indexes of silty compressibility and the pH values of contaminated silty soil was shown in Fig. 4. The curves show that when the pH value of the silty soil gradually deviates from 7.0, the value of a and C_c increase gradually, and the value of E_s decreases. In summary, the compressibility of contaminated silty soil increases with the increase in pH values deviating from 7.0.

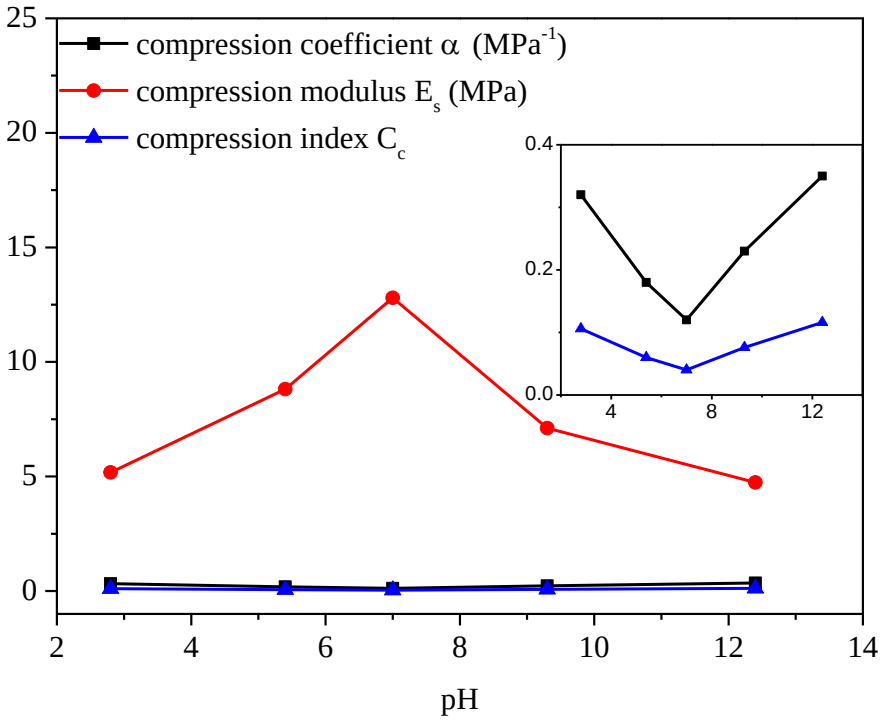

Figure 4. Compression index (α , E_s and C_c) curve of silt with various pH values (pH = 2.8, 5.4, 7.0, 9.3 and 12.4)

It can be seen from the above analysis of compressibility of contaminated silty soil, with the increasing pollution degree of silty soil, the compressibility of silty soil increased significantly. As a result, the contaminated silty soil will deformed obviously under the action of external forces which was harmful to engineering construction. Consoli and Rosa considered that water content, porosity and cement content as paramenters controlling strength of artificially cemented silty soil[50]. Therefore, for contaminated silty soil, one of the main reasons for the above results may be that the pore volume of soil increased due to the electrochemical reactions inside the silty soil. At the same time, the compressive capacity of soft plastic reaction products is relatively low.

3.2 Electrochemical properties of contaminated silty soil

Soil is composed of three phases (solid, liquid and gas). And silty soil is a conductor under normal natural conditions[36, 37]. Generally, the conductive paths in silty soil media can be divided into three types[25]. The first is a well-conductive path composed of pore fluid in silty soil. The second is an almost insulated path composed of silty particles. However, under the action of alternating current, the two end surfaces of the silty particles can be considered as a double parallel plate capacitance. Silty particles are used as the dielectric, and the flow of the current can be realized through the charge and discharge process of the capacitor[26, 27]. The third is the conductive path formed by the interface between the silty particles and the pore fluid. The ions in the pore fluid will enter the diffusion zone of the solid-liquid interface by ion exchange and migrate to the surface of the soil particles to have an electrochemical reaction. As shown in Fig.5, the various sizes of silty particles are idealized into three circles with different diameters, and the pore fluid in silty soil medium is expressed in white colour.

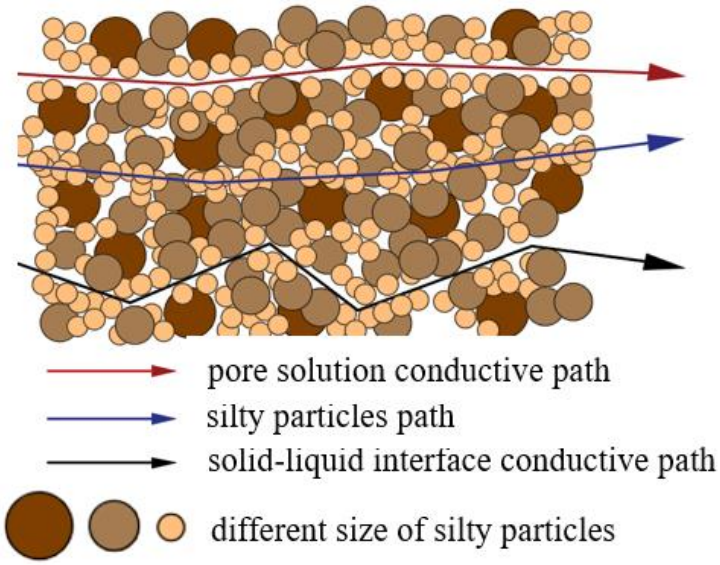

Figure 5. Conduction path of sily soil

Combined with the analysis of the conductive path, in the ideal state, there are two processes in the electrochemical system of silty soil medium. One is the charge and discharge process of electric double layer on the surface of soil particles when the electrode potential changes. The process is called the non-Faraday process[34]. The other process is the Faraday process in the diffusion zone of the solid-liquid interface at a certain electrode potential. The process consists of two parts: the charge transfer activity and the diffusion activity. Feliu et al., established a simple universal equivalent circuit with clear physical significance in the process of studying concrete[34]. Equivalent circuit model of contaminated silty soil was established through similar research methods: the two processes mentioned above are characterized by a double layer capacitance C parallel with charge transfer resistor R_t and diffusion resistance R_w. In addition, considering the conduction process of the pore fluid, a solution resistance R_s is connected in the circuit above. In the actual testing process, because of the uneven surface of the electric electrode, the double layer capacitance C has different response time

to the angular frequency, resulting in the dispersion effect of the double layer capacitance. Therefore, the constant phase angle element CPE is used to replace the double layer capacitance C in the equivalent circuit[4]. The component of CPE is controlled by two parameters, Y_{0Q} and n, respectively, in which Y_{0Q} reflects the capacitance of the double layer. And n reflects the degree of deviation of the CPE from the ideal condition. The parameter value n changes from 0 to 1. The property of CPE is close to that of the double layer capacitor C when n is very close to 1[13]. The equivalent circuit model (R_s (CPE (R_t R_w))) of the electrochemical system in contaminated silty soil is shown in Fig. 6[35].

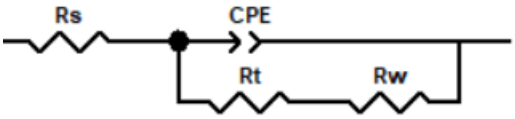

Figure 6. Equivalent circuit model of silty soil (R_s (CPE (R_t R_w)))

In the equivalent circuit shown in Fig.6, the constant phase angle component CPE can be expressed as follow[28]:

$$R_{CPE} = \frac{1}{Y_{OQ}(jw)^n} \quad (4)$$

Y_{OQ} is the admittance of the double layer capacitance, the unit is $S \cdot cm^{-2} \cdot sec^{-n}$, w is the test frequency, and j is the complex number.

The diffusion resistance R_w can be expressed as follow[29]:

$$R_w = \frac{1}{Y_{OW}(jw)^{\frac{1}{2}}} \quad (5)$$

Y_{OW} is diffusion admittance, and the unit is $S \cdot cm^{-2} \cdot sec^{-1/2}$.

The impedance of the whole electrochemical system can be expressed as follows:

$$R = R_s + \frac{1}{\frac{1}{R_{CPE}} + \frac{1}{R_t + R_w}} \quad (6)$$

The formula (4) and (5) are substituted into the formula (6):

$$R = R_s + \frac{R_t Y_{0w}(jw)^{\frac{1}{2}} + 1}{Y_{0w}(jw)^{\frac{1}{2}} + R_t Y_{0w}(jw)^{\frac{1}{2}} Y_{0Q}(jw)^n + Y_{0Q}(jw)^n} \quad (7)$$

The EIS of each group of contaminated silty soil is shown in Fig. 7. It can be seen from Fig. 7 (a) that, on one hand, the curves of each silty soil sample are Randle's curves[30], and the curves are composed of the arcs of the high frequency region and the oblique lines in the low frequency region. On the other hand, compared with the neutral silty soil (pH value is 7.0), with the continuous intervention of acid or alkaline pollutants, the intercept value of the curve and the abscissa decreases, and the radius of the arc in the high frequency region also decreases. According to the theory of EIS[31], the equivalent circuit of the simulation through the Nyquist curve is consistent with the equivalent circuit deduced previously. The intercept value of each curve and abscissa is the characterization of the solution resistance value R_s in the equivalent circuit, and the radius of the arc is related to the charge transfer resistance R_t. Therefore, a preliminary understanding of the change in the equivalent circuit elements parameters can be obtained through the Nyquist curves[47, 48]. Fig. 7(b) is

the phase angle graph. It can be seen from the figure that the phase angle values of each group fluctuate in the range of 0°~90°. According to the theory of EIS[31], the phase angle value does not reach the critical value of 0° or 90°, which indicates that the electrochemical system is both resistive and capacitive. Secondly, in the low frequency region of 10^{-2} ~ 10 Hz, the phase angle values of each group are all descending. With the increase in the test frequency, the phase angle value of each group has a peak in the frequency range of 10^{1} ~ 10^{4} Hz, which shows that only one time constant exists in the equivalent circuit.

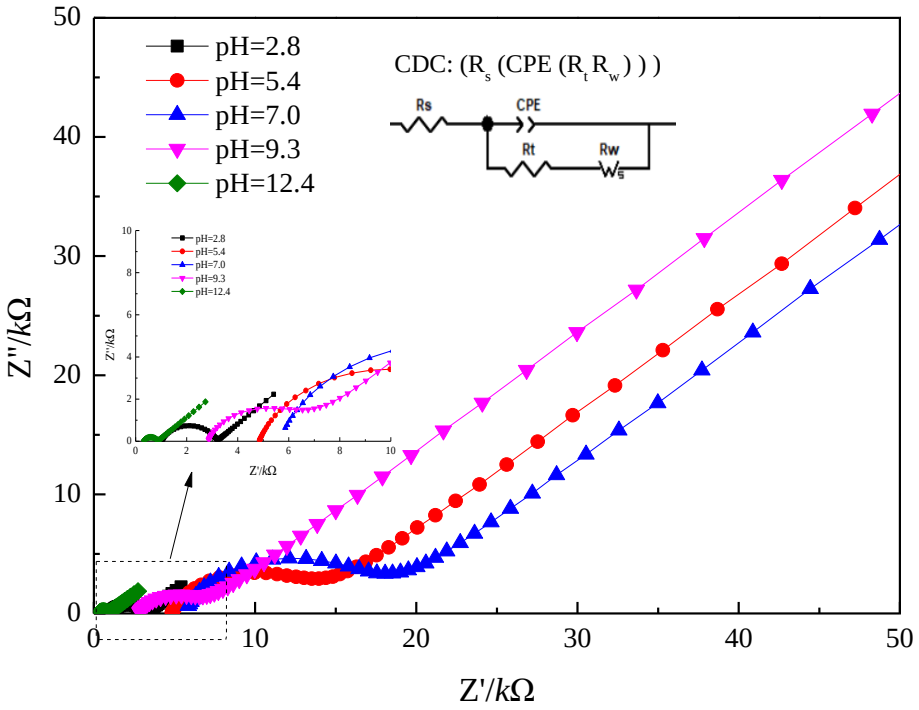

(a) Nyquist plots

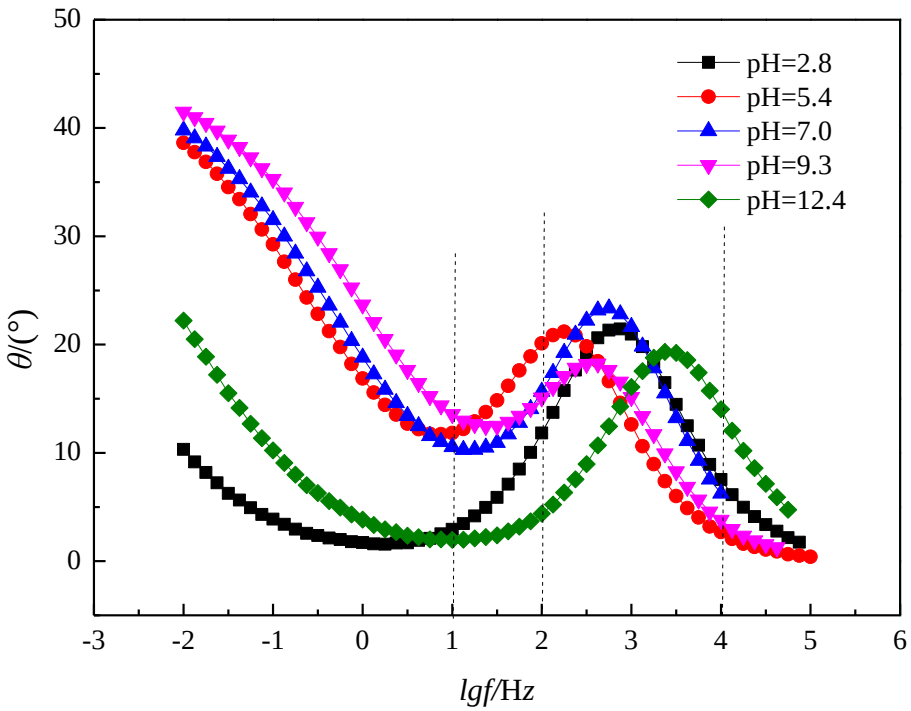

(b) Phase angle graph

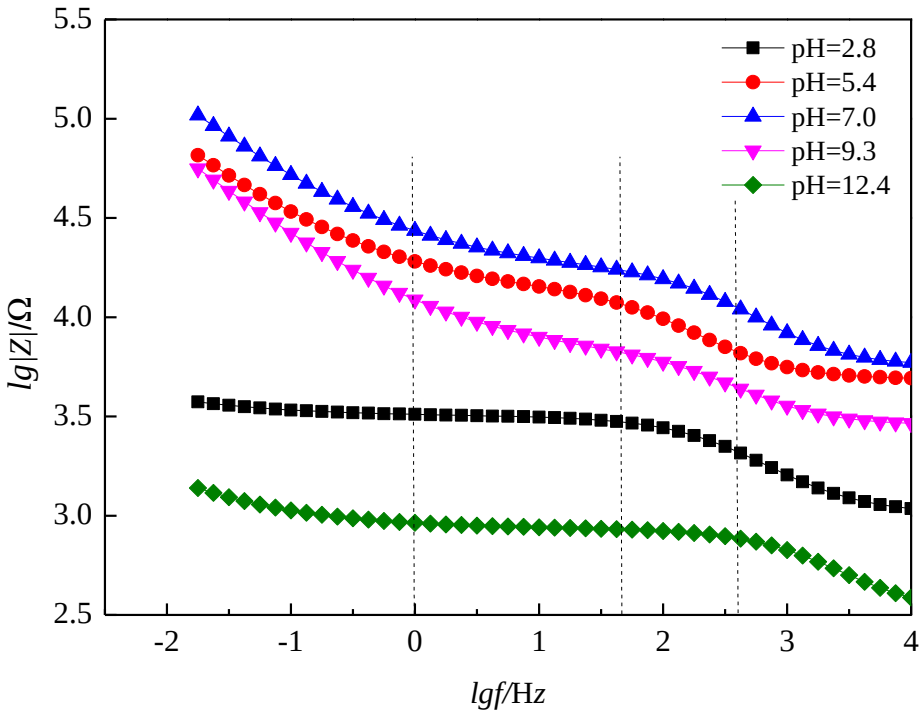

(c) Impedance mode value diagram

Figure 7. EIS diagram of H_2SO_4 and NaOH contaminated silty soil with various pH values ((a). Nyquist plots, (b). Phase angle graph, (c).Impedance mode value diagram)

Fig. 7 (c) is the line chart of the impedance modulus varying with the pH value of contaminated silty soil, which has three main characteristics: First, with the increase in test frequency, the impedance modulus |Z| of each silty soil sample continued to decline. Second, with the increase in acidic and alkaline pollutants, the impedance modulus |Z| of contaminated silty soil decreases. And third, the silty soil sample impedance modulus (|Z|) decreased greatly in the low frequency region (10^{-2} ~ 10^{0} Hz) and the middle-high frequency regions (10^{2} ~ 10^{3} Hz), but the declining trend of the low frequency region (10^{0} to 10^{2} Hz) and the high frequency region (10^{3} to 10^{4} Hz) was obviously slowed.

Table 5. Fitting parameter values of equivalent circuit (R_s (CPE (R_t R_w)))

group	pH=2.8	pH=5.4	pH=7.0	pH=9.3	pH=12.4
R_s (kΩ·cm^2)	1.01	4.84	5.62	2.84	0.32
R_t (kΩ·cm^2)	2.17	8.75	12.01	3.81	0.54
Y_{OQ} (μS·cm^{-2}·sec^{-n})	1.41	0.68	0.21	0.72	1.53
n	0.76	0.79	0.80	0.81	0.78
Y_{OW} (μS·cm^{-2}·sec$^{-1/2}$)	400	53.8	22.81	58.11	476

The equivalent circuit (R_s (CPE (R_t R_w))) was fitted by Zsimpwin software, and the fitting parameters of each electrochemical components in the equivalent circuit are listed in Table 5[49]. It can be seen from Table 5 that the solution resistance R_s and the charge transfer resistance R_t increase with the degree of contaminated silty soil deviating from 7.0 of pH values. In addition, the double layer admittance Y_{OQ} and the diffused admittance Y_{OW} are inversely proportional to the impedance and decrease with the degree of contaminated soil deviating from 7.0 of pH values. The variation trend of the line chart shows that the diffusion admittance Y_{OW} and the charge transfer resistance R_t change considerably with the increase in acidity or alkalinity of the contaminated silty soil, especially the diffusive admittance Y_{OW}. When pH value reaches 2.8 or 12.4, Y_{OW} increases approximately 18 times relative to the 7.0 pH value. However, the change in acid or alkaline content of the contaminated silty soil has little effect on the double layer admittance Y_{OQ}. The solution resistance R_s showed a slight decrease with the continuous intervention of acidic or alkaline pollutants. From the above analysis, it can be seen that the equivalent circuit elements used to simulate the internal structure of silty soil have changed in varying degrees. Which indicates that with the continuous intervention of acid-base pollutants, a series of electrochemical reactions have occurred in silty soil media[39]. According to the variation of the components, the electrochemical reactions in the contaminated silty soil are mainly include diffusion and charge transfer processes. The diffusion resistance of ions in pore fluid decreases, therefore, the electrochemical reaction is more and more likely to occur. At the same time, the charge transfer on the surface of the silty particles is more frequent, which made the silty soil internal structure disturb in a certain extent, and eventually the properties of silty soil changed due to the contamination[41, 42].

3.3 Relationship between mechanical and electrochemical properties

As discussed in Sections 3.1 and 3.2 above, the mechanical and electrochemical properties of contaminated silty soil show a certain regularity. Changes in mechanical properties (shear strength and compressibility) of contaminated silty are due to electrochemical reactions resulting from the continuous intervention of acid-base contaminants[36]. Therefore, the electrochemical method is one of the most effective and fundamental methods to study the mechanical properties of contaminated silty soil[46]. Tao and Gao have study the compressive strength of concrete based on Electrochemical Impedance Spectroscopy. The phase angle of concrete was suitable for assessing the compressive strength of concrete[46]. For contaminated silty soil, from the previous analysis of the equivalent circuit components of the EIS, it is known that the diffusive admittance Y_{OW} and charge transfer resistance R_t vary significantly with the pH value of contaminated silty soil. Among them, the shear strength of silty soil is directly proportional to R_{ct} and inversely proportional to $Y_{ow.}$ The compressibility of silty soil is inversely proportional to R_{ct} and proportional to $Y_{ow.}$ The diffusion process and the charge transfer process correspond to the third conductive paths that were formed by the interface between the silty particles and the pore fluid. With the continuous intervention of H_2SO_4 and NaOH, the increase in diffusive admittance Y_{OW} indicates that the resistance of the ions in the pore fluid of silty soil to the diffusion region decreases. An increasing number of positively charged cations enter the diffusion region of the solid-liquid interface under the action of ion exchange[37]. The number of ions in the diffusion region is increased. Simultaneously, the charge transfer resistance R_t decreases, which makes more ions migrate to the surface of silty particles. The process of migration is accelerated by the drive of potential power[44], and the electrochemical reaction process becomes easier. The electrochemistry reaction is carried out through the migration activity on the surface of silty particles, and the charge transfer is completed. In the process of electrochemical reaction, some of the minerals (such as SiO_2, Fe_2O_3, Al_2O_3 and CaO) in silty soil media become soft plastic products (such as Na_2SiO_3, $NaFeO_2$, $NaAlO_2$ and Fe_2S_3)[33]. The volume of soft plastic products in silty soil is several times that of mineralas, therefore, the volume of contaminated silty soil expand to a certain extent. The pore size of silty soil has increased; as a result, the compressibility of silty soil has also increased. In addition, various organic and inorganic cementing materials between silty particles are dissolved, and the connection between silty particles is weakened[33]. The shear strength of silty soil is considerably reduced.

4. CONCLUSION

By analysing the mechanical and electrochemical experiment results of H_2SO_4 and NaOH contaminated silty soil, the following conclusions can be obtained.

(1) According to the results of the mechanical test, the shear strength decreased and compressibility increased gradually with the pH value of contaminated silty soil continuously deviating from pH 7.0.

(2) The results of the electrochemical experiment show that the diffusion admittance Y_{OW} and the double layer admittance Y_{OQ} increased with the increase in acid-base silty soil, and while the

solution resistance R_s and charge transfer resistance R_t gradually decreased. The diffusive admittance Y_{OW} and charge transfer resistance R_t vary greatly.

(3) It is known from the comparison between the mechanical experiment and the electrochemical experiment results that with the increase in acidity or alkalinity of silty soil, the change in mechanical properties of contaminated silty soil is mainly caused by the decrease in the resistance of the charge transfer process and diffusion process of the pore liquid ions in the silty soil medium, and the electrochemical reaction becomes easier. In the process of electrochemical reaction, some of the minerals (such as SiO_2, Fe_2O_3, Al_2O_3 and CaO) in silty soil media become soft plastic products (e.g., Na_2SiO_3, $NaFeO_2$, $NaAlO_2$ and Fe_2S_3). Simultaneously, various organic and inorganic cementing materials between silty particles are dissolved, and the connection between silty particles is weakened. As a result, the compressibility of silty soil increase and the shear strength reduced considerably. Therefore, the diffusion admittance Y_{OW} and charge transfer resistance R_t can be used to evaluate the mechanical properties of contaminated silt soil.

ACKNOWLEDGEMENTS

This work was supported by the National Natural Science Foundation of China (No.51208333 and 51501125), the China Postdoctoral Science Foundation (No.2012M520604 and No.2016M591415), the Natural Science Foundation for Young Scientists of Shanxi Province (No.2013021013-2, No.2014011036-1, No.2014011015-7) the Science and Technology Programs for Research and Development of Shanxi Province (No.2013KJXX-08), the program for State Key Laboratory of Hydraulic Engineering Simulation and Safety of Tianjin University (HESS1613).

References

1. Abdel Salam Hamdy, E. El-Shenawy and T. El-Bitar, *Int. J. Electrochem. Sci.*, 1 (2006) 171.
2. N. Ehteram A and Aisha H. Al-Moubaraki, *Int. J. Electrochem. Sci.*, 3 (2008) 806.
3. C. A. Ferreira, J. A. Ponciano, D. S. Vaitsman and D. V. Perez, *Sci. Total Environ.*, 388 (2007) 250.
4. P. J. Han, *Int. J. Electrochem. Sci.*, 11 (2016) 9491.
5. M. Jeannin, D. Calonnec, R. Sabot and P. Refait, *Corros. Sci.*, 52 (2010) 2026.
6. S. Marcelin, N. Pébère and S. Régnier, *Electrochim. Acta*, 87 (2013) 32.
7. M. Maslehuddin, M. M. Al-Zahrani, M. Ibrahim, M. H. Al-Mehthel and S. H. Al-Idi, *Constr. Build. Mater.*, 21 (2007) 1825.
8. P. Morales Gil, *Int. J. Electrochem. Sci.*, 13 (2018) 3297.
9. E. A. Noor and A. H. Al-Moubaraki, *Arab. J. Sci. Eng.*, 39 (2014) 5421.
10. Ping Liang, Cui-wei Du, Xiao-gang Li, Xu Chen and Zhang liang, *Int. J. Min. Met. Mater.*, 16 (2009) 407.
11. B. He, P. J. Han, L. Hou, D. Zhang and X. H. Bai, *Eng. Fail. Anal.*, 80 (2017) 325.
12. B. He, P. J. Han, C. Lu and X. H. Bai, *Eng. Fail. Anal.*, 58 (2015) 19.
13. P. J. Han, *Int. J. Electrochem. Sci.*, 12 (2017) 7668.
14. N. Otsuki, W. Yodsudjai and T. Nishida, *Constr. Build. Mater.*, 21 (2007) 1046.
15. J. Y. Huang, Y. B. Qiu and X. P. Guo, *Mater. Corros.*, 60 (2009) 527.
16. A. Legat. *Electrochim. Acta*, 52 (2007) 7590.
17. S. Li, S. Jung, K. Park, S. M. Lee and Y. G. Kim, *Mater. Chem. Phys.*, 103 (2007) 9.
18. M. Mckenzie and P. Vassie, *Brit. Corros. J.*, 20 (1985) 117.
19. N. Naing Aung and Y. J. Tan, *Corros. Sci.*, 46 (2004) 3057.
20. F. Hass, A. C. Abrantes, A. N. Diógenes and H. A. Ponte, *Electrochim. Acta*, 124 (2014) 206.

21. H. Sun, Z. Ren, S. A. Memon, D. Zhao, X. Zhang, D. Li and F. Xing, *Constr. Build. Mater.*, 135 (2017) 361.
22. B. James and T. Tamtsia, *J. Adv. Concr. Technol.*, 2 (2004) 113.
23. S. Zhang, *Int. J. Electrochem. Sci.*, 13 (2018) 3246.
24. B. Yuan. *Int. J. Electrochem. Sci.*, 12 (2018) 3396.
25. P. J. Han, Y. F. Zhang, F. Y. Chen and X. H. Bai, *J. Cent. South Univ.*, 22 (2015) 4318.
26. G. Song. *Cement Concrete Res.*, 30 (2000) 1723.
27. G. Qiao, Y. Hong, J. Ou and X. Guan, *Measurement*, 67 (2015) 84.
28. G. Qiao, Y. Hong and J. Ou, *Measurement,* 67 (2015) 78.
29. G. Qiao, B. Guo, Z. Li, J. Ou and Z. He, *Constr. Build. Mater.*, 134 (2017) 388.
30. D. A. Harrington and P. V. Driessche, *Electrochim. Acta*, 56 (2011) 8005.
31. C. N. Cao, Principles of Electrochemistry of corrosion, Beijing Industrial Press (2008) Beijing, China.
32. T. H. Wu, Soil Mechanics, Allyn and Bacon (1977), China.
33. B. M. Das, Adanced Soil Mechanics, Soft Clay Engineering (1981), UK.
34. V. Feliu, J. A. Gonzalez and C. Andrade, *Corros. Sci.*, 39 (1998) 846.
35. V. Feliu, J. A. Gonzalez and C. Andrade, *Corros. Sci.*, 40 (1998) 995.
36. M. M. Yan, L. C. Miao and Y. Cui, *Mar. Georesour. Geotec.*, 30 (2012) 167.
37. X. Q. Dong, G. H. Yang, X. H. Bai and Y. K. Lv, *ADV. Mater.,* 287 (2011) 815.
38. L. H. Han, S. Y. Liu and Y. J. Du, *Chinese Journal of Geotechnical Engineering*, 28 (2006) 1028.
39. K. Wang and M. J. Zhao, *ADV. Mater.*, 726 (2013) 3877.
40. M. Zhou, J. G. Wang, S. B. Huang, P. Dou and L. Q. Zhang, *Rock & Soil Mechanics*, 32 (2011) 3269.
41. P. Gu, P. Xie and J. J. Beaudoin, *Cenment Concrete Res.*, 23 (1993) 581.
42. Jose Augusto de Lollo, Roger Augusto Rodrigues, Vagner Roberto Elis and Renato Prodo, *Bull. Eng. Geol. Environ.* 70 (2011) 299.
43. T. Islam, Z. Chik, M. M. Mustafa and H. Sanusi, *Environ. Earth Sci.*, 67 (2012) 1299.
44. Bohni H., Corrosion in Reinforced Concrete Structure, China Machine Press (2009) China.
45. Moavedi Hossein, Kazemian Sina and Huat Bujang, *Int. J. Electrochem. Sci.*, 7 (2012) 7740.
46. Guilan Tao, Congong Gao, Zhaoyang Qiao, *Int. J. Electrochem. Sci.*, 12 (2017) 11629.
47. B. Dong, Q. Qiu, J. Xiang, C. Huang, F. Xing and N. Han, *Materials.*, 7 (2014) 218.
48. Z. Yang, J. Hollar and X. Shi, *J. Mater. Sci.*, 45 (2010) 3497.
49. J. L. Marriaga, C. Higuera and P. Claisse. *Constr. Build. Mater.*, 52 (2014) 9.
50. N. C. Consoli, A. R. Daniela, C. C. Rodrigo, A. D. Rosa, Eng. Geol., 122 (2011) 328